Numerical Study of Atmospheric Icing on Non Rotating Circular Cylinders in Tandem Arrangement

Muhammad Virk

Reprinted from

The Journal of
Computational Multiphase Flows

Volume 5 · Number 1 · 2013

Multi-Science Publishing

Numerical Study of Atmospheric Icing on Non Rotating Circular Cylinders in Tandem Arrangement

Muhammad S. Virk
Department of Technology, Narvik University College, Norway

Received: 15June 2012, Accepted: 4 January 2013

Abstract
Numerical study of atmospheric ice accretion on two non-rotating circular cylinders in tandem arrangement was carried out at different operating and geometric conditions. To validate the numerical model, initially the results of ice accretion on single circular cylinder were compared with the experimental data obtained from CIGELE atmospheric icing research wind tunnel (CAIRWT) [1, 2]. A good agreement was found between experimental and numerical results. Numerical analyses of ice accretion on two circular cylinders in tandem arrangement showed that accreted ice loads decreases with the increase in distance between the cylinders and also affects the rate and shape of ice accretion. Parametric study at different droplet sizes and temperatures showed a significant change in ice accretion. This research work provides a useful base for better understanding and further investigation of atmospheric ice accretion on circular overhead power network cables in tandem arrangement, installed in the cold regions.

Keywords: Atmospheric ice, circular cylinder, droplet size distribution, distance, temperature.

1. INTRODUCTION

Atmospheric icing is the term used to describe the ice accretion on structures and understanding of the problems related to this are of interest to engineers and scientists. Depending on the ice type, the atmospheric ice can be classified as: *rime, glaze or mixed ice*[3]. Atmospheric ice accretion occurs, when freezing rain drops, snow particles or super cooled water droplets come into contact with the exposed structural surface [1]. The potential damage to facilities as a result of atmospheric ice accretion is considerable. Numerical study of atmospheric ice accretion on circular cylinders in tandem arrangement include the computation of mass flux of icing particles as well as determination of the icing conditions [4]. This can be numerically simulated by means of integrated thermo-fluid dynamic models, where icing conditions can be defined by the heat balance on the iced surface. Various numerical studies related to the atmospheric icing on structures can be found in literature. The first attempts were made in 1980's to obtain data for generating ice shapes on various shape structures. In 1983 Lozowski et al. [5] presented a numerical model to simulate the ice accretion process on an unheated, non-rotating cylinder for rime and glaze ice conditions. In 1984, Makkonen [6] proposed a numerical model to reveal the relationship between the accreted ice loads and relevant metrological parameters. In these models Makkonen and Lozowski assumed the thermodynamic conditions and the initial icing rate to be a function of the angle around the upstream face of the cylinder and were computed using classical Messinger equation [1].

This paper describes the CFD based numerical study of atmospheric ice accretion on two non-rotating circular cylinders in tandem arrangement. To understand the basics of ice accretion, initial numerical analyses were done using a single circular cylinder and the results were published by authors [2]. In this research work a detailed numerical study is carried out to understand and simulate the atmospheric ice growth on two circular cylinders in tandem arrangement at different operating and geometric conditions.

*Corresponding Author: E-mail address: Email: msv@hin.no

2. NUMERICAL SETUP

Numerical modeling of atmospheric icing on circular cylinders involves the fluid flow simulation, droplet behavior, surface thermodynamics and phase change. CFD based numerical analyses were carried out using a finite element based technique [7], where 2D problem is solved in 3D by considering a single cell layer in the span wise longitudinal direction of each cylinder. A Z-symmetry boundary condition is then imposed on side. Air flow was simulated by using the Navier Stokes equations.

$$\frac{\partial \rho_a}{\partial t} + \vec{\nabla}.\left(\rho_a \vec{V}_a\right) = 0$$

$$\frac{\partial \rho_a \overrightarrow{V_a}}{\partial t} + \vec{\nabla}.\left(\rho_a \overrightarrow{V_a}\overrightarrow{V_a}\right) = \vec{\nabla}.\sigma^{ij} + \rho_a \vec{g}$$

$$\frac{\partial \rho_a E_a}{\partial t} + \vec{\nabla}.\left(\rho_a \overrightarrow{V_a} H_a\right) = \vec{\nabla}.\left(k_a\left(\vec{\nabla} T_a\right) + v_i \tau^{ij}\right) + \rho_a \vec{g}.\overrightarrow{V_a} \tag{1}$$

$$\sigma^{ij} = -\delta^{ij} p_a + \mu_a [\delta^{jk}\nabla_k v^i + \delta^{ik}\nabla_k v^j - \frac{2}{3}\delta^{ij}\nabla_k v^k] = -\delta^{ij} p_a + \tau^{ij}$$

where σ^{ij} is the stress tensor, k is the thermal conductivity, E is the internal energy, whereas H is the enthalpy, subscript 'a represents air in equation 1. C-type structured numerical grid was used (figure-1). For this study 450,000 mesh elements were used, where to capture the boundary layer characteristics (shear stresses and heat fluxes) accurately, y+ value less than 1 was used near the wall. Number of mesh elements and y+ value was selected based upon the heat flux calculations, where a numerical check was imposed that the heat flux computed with the classical formula dT/dn should be comparable with the heat flux computed with the Gresho's method.

The sand grain roughness height for the iced surface was calculated with an empirical NASA correlation described by Shin et al. [8, 9]. The corresponding value of the sand grain roughness is obtained from:

$$K_s = 0.6839 \left[\frac{K_s/C}{\left(K_s/C\right)_{base}}\right]_{LWC} \left[\frac{K_s/C}{\left(K_s/C\right)_{base}}\right]_{T_S} \left[\frac{K_s/C}{\left(K_s/C\right)_{base}}\right]_{MVD} \left(K_s/C\right)_{base} c \tag{2}$$

$$\left[\frac{K_s/C}{\left(K_s/C\right)_{base}}\right]_{MVD} = \begin{cases} 1 & \text{MVD} \le 20 \\ 1.667 - 0.0333(MVD) & \text{MVD} \ge 20 \end{cases}$$

$$\left[\frac{K_s/C}{\left(K_s/C\right)_{base}}\right]_{LWC} = 0.5714 + 0.2457(LWC) + 1.2571(LWC)^2$$

$$\left[\frac{K_s/C}{\left(K_s/C\right)_{base}}\right]_{T_S} = 0.04T_S - 11.27$$

where MVD is the droplet mean diameter, $\left({K_s}/{C} \right)_{basi}$ = 0.001177. The one equation Spalart Allmaras turbulence model was used as a compromise between acceptable computational cost and the required accuracy in simulating the turbulent flow. Two phase flow (air & water) was solved using Eulerian-Eulerian approach, where super cooled water droplets were assumed to be spherical. The Eulerian two phase fluid model consists of the Navier-Stokes equation, augmented by the water droplets continuity and momentum equation. The water droplet drag coefficient is based on the empirical correlation for the flow around the spherical droplets described by Clift et al. [10].

$$\frac{\partial \alpha}{\partial t} + \vec{\nabla}.\left(\alpha \vec{V}_d\right) = 0$$

$$\frac{\partial\left(\alpha \vec{V}_d\right)}{\partial t} + \vec{\nabla}.\left(\alpha \vec{V}_d.\vec{V}_d\right) = \frac{C_D \operatorname{Re}_d}{24K}\alpha\left(\vec{V}_a - \vec{V}_d\right) + \alpha\left(1 - \frac{\rho_a}{\rho_d}\right)\frac{1}{Fr^2}\vec{g}$$

$$K = \frac{\rho_d d^2 v_{a,\alpha}}{18 L_\alpha U_a} \quad , \quad Fr = \frac{v_{a,\alpha}}{\sqrt{L_\alpha g}} \quad , \tag{3}$$

$$\operatorname{Re}_d = \frac{\rho_d d v_{a,\alpha} \left\| v_a - v_d \right\|}{\mu_a}$$

where α is the water volume fraction in air flow, V_d is the droplet velocity, V_a is the air velocity, C_D is the droplet drag coefficient and Fr is the Froude number. Droplet collection efficiency on cylinder surface is calculated at every surface point using [11]:

$$\beta = -\alpha u.n \tag{4}$$

where 'n' is the surface normal. The water flux at the surface is calculated by:

$$m_w = LWC.U_\infty.\beta \tag{5}$$

Surface thermodynamic and icing rate are calculated by using the mass and energy conservation equations, considering the heat fluxes due to convective cooling, evaporative cooling, heat of fusion, viscous heating, kinetic heating and solar radiation [12].

$$Q_{in}^o = Q_{out}^o \tag{6}$$

$$Q_{latent\ \text{heat}} + Q_{\text{aerodynamic heat}} + Q_{\text{KE heat}} = Q_{\text{sublimative heat}} + Q_{\text{convective heat}} + Q_{\text{droplet,cooling heat}} + Q_{\text{radiative heat}}$$

Where

$$Q_{\text{aerodynamic,heating}} = \frac{\text{r}h_c v_\alpha^2}{2C_p}$$

r = Adiabatic recovery factor , (r = $P_r^{1/2}$ for laminar and r = $P^{1/3}$ for turbulent flow)

C_p = Specific heat of air , 1006 J/kgK

h_c =Convective heat transfer coefficient

$Q_{latent,heat} = (LWC.\beta.v_{\alpha}).\lfloor L_f + C_i(T_{air} - T_{surface}) \rfloor$

C_i = Specific heat of ice

L_f =Latent heat of fusion

$Q_{droplrt,kinetic,energy} = (LWC.\beta.v_{\alpha})\frac{v_{\alpha}^2}{2}$

$Q_{convection} = h_c(T_{surface} - T_{air})$

$Q_{sublimation} = \chi_s e_o (T_{surface} - T_{air})$

$\chi_s = \frac{0.622 h_c L_s}{C_p P_t L_e^{0.66}}$

e_o = 27.03

L_S = Latent heat of sublimation.

L_e =Lewis number, $1/P_r$

P_t = Total pressure of air

$Q_{droplet,cooling} = \rho_a \beta v_{\alpha} C_{p,w}(T_{surface} - T_{air})$

$C_{p,w}$ = Specific heat of water , 4218 J/kgK

$Q_{radiation} = 4\varepsilon\beta_r T_{air}^3 (T_{surface} - T_{air})$

ε= Surface emisivity , 0.5 - 0.8

σ_r = Stephan boltzman constant, 5.6704 x 10^{-8}

Ice density was calculated by using the Jones formula, defined as:

$$R_M = -\frac{d.\left\|\vec{V_d}\right\|}{2T_{wall}}$$

$$\rho_{ice} = \begin{cases} 0.21 R_M^{0.53} & R_M \le 10 \\ R_M / (1.15 R_M + 2.94) & 10 \le R_M \le 60 \\ 0.84 & R_M \ge 60 \end{cases} \quad (7)$$

Coupled ALE (Arbitrary Langrangian Eulerian) formulation was used for the mesh displacement due to ice accretion in time. This approach adds the grid speed terms to the Navier-Stokes equations to account for the mesh velocity[9]. The coupled ALE method solves for the mesh displacements in the x-, y-, and z-direction simultaneously, providing a better distribution of the effect of meshed iced surface displacement into the interior of the computational domain. This approach yields good mesh orthogonality and element quality near the surface. The numerical simulations were carried out at the operating and geometric conditions specified in Table-1.

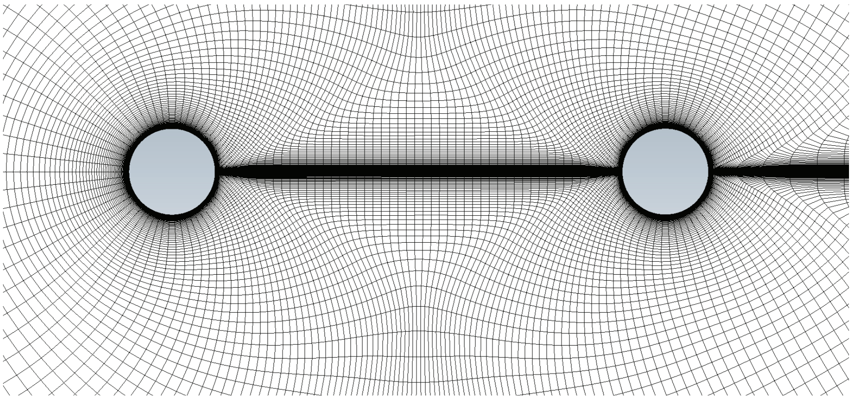

Figure 1. C-Type Structured Numerical Grid

Table 1: Operating conditions used for the simulations

Free Stream Wind Velocity [m/s]	5
Droplet Size , MVD [µm]	20, 30, 35
Tandem Arrangement Distances [m]	0.2, 0.4, 0.6
Liquid Water Content , LWC [g/m^3]	1.2
Atmospheric Air Temperatures [°C]	-2.5, -7.5, -15
Simulation Time [minutes]	30
Cylinder Diameter [m]	0.035
Cylinder longitudenal length [m]	0.005

3. MODEL VALIDATION

Initial analyses were carried out on single circular cylinder to validate the numerical data with the experimental tests carried out in the CIGELE atmospheric icing research wind tunnel (CAIRWT), at v = 5 m/sec , MVD= 35 µm, T= -15C and conductor diameter of 35 mm. This experimental data was obtained from the research article published by Ping Fu et al. [1] in 2006. Figure 2 shows the comparison of accreted ice shapes obtained from this numerical study and experimental study from Ping Fu et al. [1, 2].

A good agreement was found between both numerical and experimental results. After the validation of model, further parametric numerical analyses were carried out considering two circular cylinders in tandem arrangement at different operating and geometric conditions.

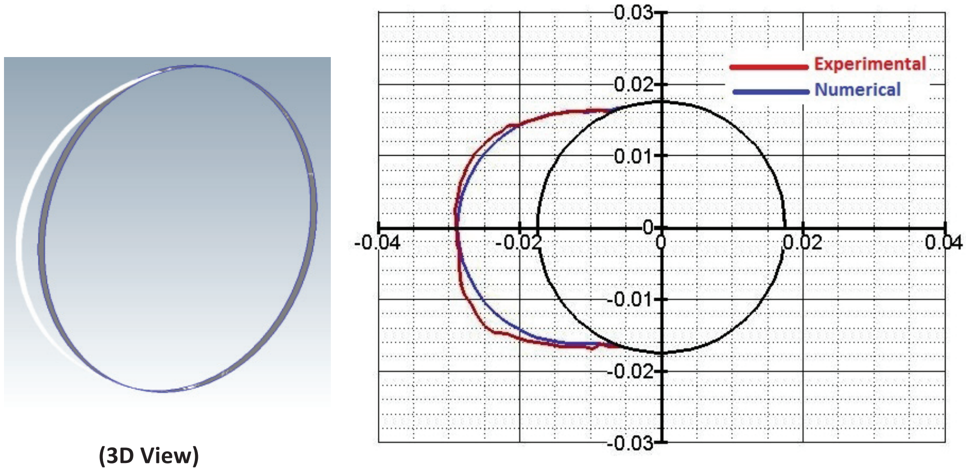

Figure 2. Comparison of accreted ice shape, obtained from numerical simulations with experiments, at v=5 m/sec, MVD= 35µm, T=-15C & t= 30 min.[2]

4. ICE ACCRETION IN TANDEM ARRANGEMENT

4.1. Effect of Distance Variation

Tandem arrangement of the circular cylinders has an effect on the rate and shape of ice accretion. Distance between cylinders is an important factor in this regard, as it affects the airflow and droplet behavior. To analyze the effect of distance variation between two cylinders in tandem arrangement, analyses were carried out considering three different distance values (200, 400 & 600 mm). Analyses show that with the increase in distance between cylinders, the droplet collision efficiency on the rear cylinder decreases, as more droplets follow the streamline after passing over the front cylinder. In case of distance= 200 mm, after passing over the front cylinder more droplets collide with the rear cylinder surface, due to the air flow behavior, as it does not get enough time to get settle, whereas in case of distance = 600 mm, air flow get settled before it reaches to the rear cylinders. Figure-3 shows the flow behavior and ice accretion on both cylinders in each case. Results show an abrupt ice shape on rear cylinder in case of 200 mm, because of air flow pattern as it does not get settled and droplets do not collide evenly across the cylinder surface and mainly collide at certain surface area, whereas in case of 600 mm results show a smooth ice shape at rear cylinder due to settle flow behavior and even collision of droplets along the cylinder surface. As an overall study showed a decrease in the accreted ice loads and thickness with the increase of distance between two circular cylinders.

4.2. Effect of Droplet Size Distribution

For numerical modeling of atmospheric icing, appropriate distribution of water droplet diameter in the air is very important. Droplet diameters in air are not uniformly distributed and can be numerically described via droplet spectra stating the fractions of the individual droplet diameters [4, 13]. To study the effect of droplet size variation on the rate and shape of ice accretion on circular cylinders in tandem arrangement, the numerical analyses were carried out for three different spherical droplet sizes with MVD of 20, 30 and 35 µm, for distance = 400 mm between cylinders. Analyses showed that increasing the droplet size increases the area covered by the accreted ice on each cylinder and consequently affects the accreted ice growth and shape. The main reason for this can be explained by the fact that larger diameter droplets have larger inertia compared to smaller droplets, therefore the movements of larger droplets are less affected by the airflow and more of the droplets collide with the cylinder surface. Results showed a smooth distribution of droplet collision at the front cylinder in each case; whereas an abrupt and uneven distribution of droplet collision is observed at rear cylinder, which is mainly due to the air flow behavior. Figure-4 shows the droplet collision efficiency along front and rear cylinder for each droplet size.

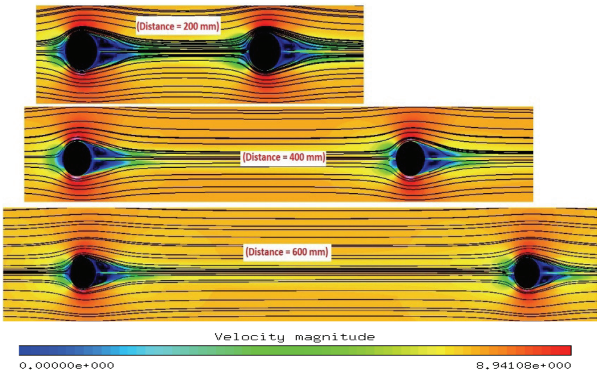

(Velocity streamlines)

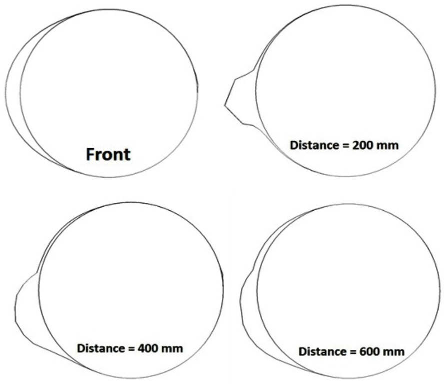

(Accreted ice shapes)

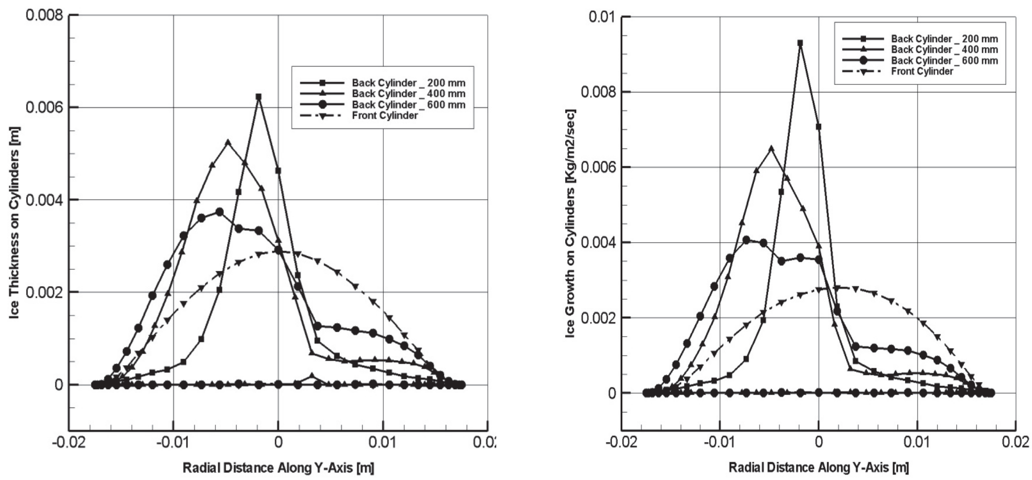

Figure 3. Effect of distance variation between cylinders on rate and shape of accreted ice.

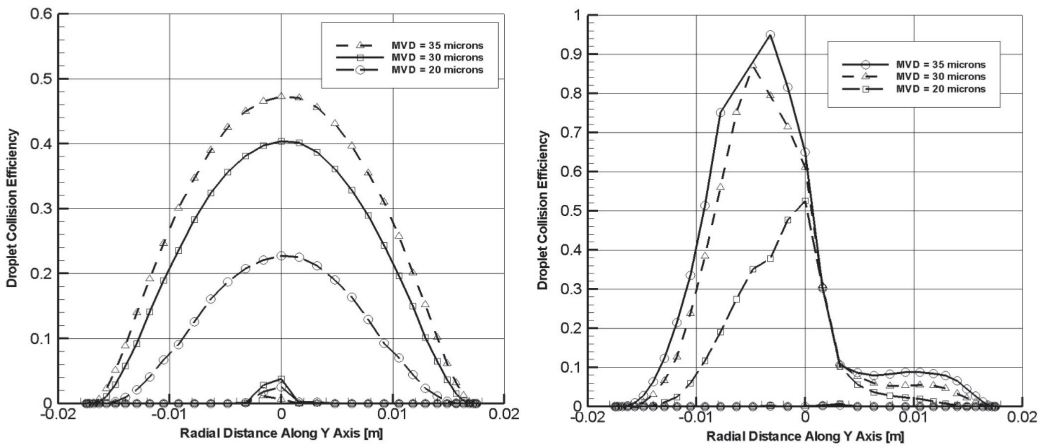

(Front conductor) (Rear conductor)

Figure 4. Droplet collision efficiency along front and rear cylinders in tandem arrangement.

Analyses showed that change in the droplet size affects both the rate and shape of ice accretion on both cylinders. Results showed a uniform ice growth on the front end cylinder; whereas an abrupt ice growth is observed at rear end cylinder. In case of less distance (200 mm) between cylinders, the droplets will hit with the rear cylinder unevenly, whereas in case of large distance between cylinders (600 mm), more smooth distribution of droplets is observed. As an overall results showed a decrease in the accreted ice load with the decrease of the droplet size in all three cases. Figure-5 shows the rate of ice accretion and resultant accreted ice thickness in case of 400 mm distance, with the change in the droplet sizes on each conductor in tandem arrangement.

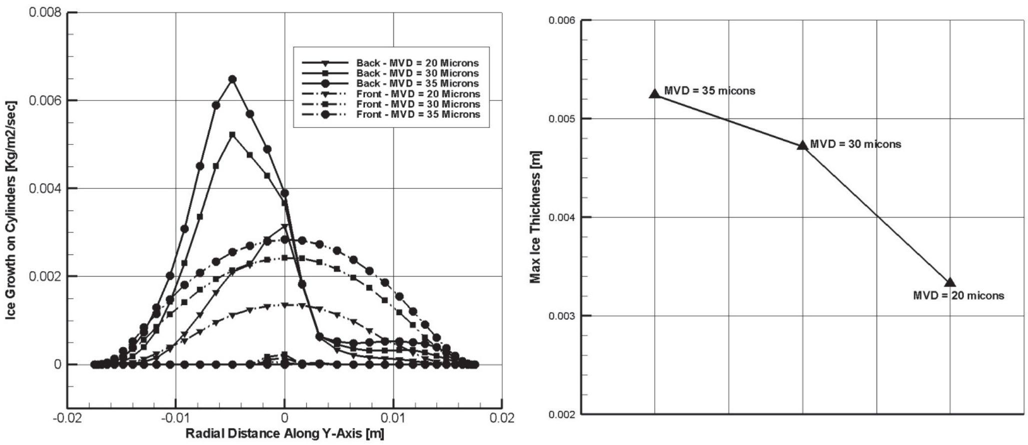

Figure 5: Effect of droplet size on ice growth on two circular cylinders in tandem arrangement, d = 400 mm.

4.3. Effect of Temperature Variation

To study the effect of atmospheric temperature variations on the rate and shape of ice accretion on circular cylinders in tandem arrangement, parametric analyses were carried out at three different atmospheric temperatures (-2.5 °C, -7.5 °C and -15 °C) at a constant median volume diameter (MVD) of 35 µm and distance of 400 mm. Results show that the accreted ice load and shape on each cylinder changes with the temperature. At -7.5 °C and -15 °C, the accreted ice shape is smoother on both cylinders, while for -2.5 °C, an abrupt ice shape is found due to wet icing conditions and water runback over the cylinder surface. At -2.5 °C the freezing fraction of water droplets hitting with the surface is low, due to which water runs back on the cylinder surface and leads to abrupt ice shapes. Figure-6 shows the accreted ice shapes on front and rear cylinder for three different temperatures at d = 400 mm.

5. FINDINGS

This research study provided the useful base information to understand the atmospheric ice accretion physics and effect of various operating parameters on two circular cylinders installed in tandem arrangement. Following are some important findings of this research work.

- Distance between the circular cylinders in tandem arrangement effects the ice growth on each cylinder. Analyses showed a smooth ice shape on front cylinder; whereas an abrupt ice shape is found on rear cylinder due to change in flow and droplet behavior. As an overall results showed a decrease in accreted ice load and thickness with the increase of the distance between the two circular cylinders in tandem arrangement.
- Change in the droplet size significantly changes the ice growth. Analyses showed a decrease in the accreted ice load and thickness on circular cylinders with the decrease of the droplet size.
- Change in atmospheric temperature affects the rate and shape of accreted ice. Analyses showed more smooth ice shape at low temperatures, whereas near freezing temperature more abrupt ice shapes are observed, due to low freezing fraction and water runback.

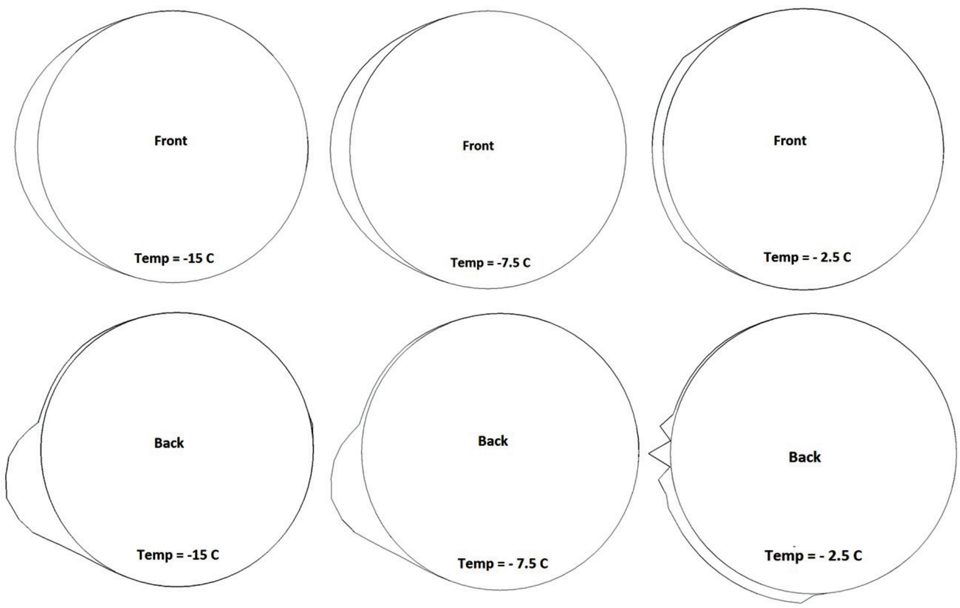

Figure 6. Effect of temperature variation on ice growth on two cylinders in tandem arrangement, d= 400mm.

ACKNOWLEDGMENT

The work reported in this paper was partially funded by the Research Council of Norway, project no. 195153/160 and partially by the consortium of the project ColdTech- Sustainable Cold Climate Technology.

REFERENCES:

[1] Ping Fu, Masoud Farzaneh, and G. Bouchard., *Two dimensional modelling of the ice accretion process on transmission line wires and conductors*. Cold region science & technology, 2006. **46**: p. 132-146.

[2] Virk, M.S., *Atmospheric Ice Accretion on Non-Rotating Circular Cylinder.* The Journal of Computational Multiphase Flows, 2011. **3**(4): p. 197-205.

[3] Cao Y, Q Zhang, and J. Sheridan. *NUMERICAL SIMULATION OF ICE ACCRETION ON AIRFOILS*. in *XXII ICTAM*. 2008. Adelaide, Australia.

[4] T Wagner, U. PEil, and C. Borri, *Numerical investigation of conductor bundle icing*, in *EACWE 5*. 2009: Florence, Italy.

[5] E P Lozowski, J R Stallabrass, and F.P. Hearty., *The Icing of anunheated, Non-rotating Cylinder, Part I: A Simulation Model*. Journal of Climate and Applied Meteorology, 1983. **22**: p. 2053-2062.

[6] Makkonen, L., *Modelling of ice accretion on wires*. Journal of climate appl, Metoer, 1984. **23**: p. 929-939.

[7] http://www.newmerical.com/index.php/products/fensap-ice-cfd-software/.

[8] J Shin and T.H. Bind., *Experimental and computational ice shapes and resulting drag increase for a NACA 0012 airfoil*. 1992, NASA technical memorandum 105743.

[9] Manual, N.S.U. 2010, NTI.

[10] R Clift, J R Grace, and M.E. Weber, *Bubbles, Drops and Particles*. 1978, New York: Academic Press.

[11] Boutanios, Z., *An Eulerian 3D analysis of water droplets impingement on a Convair-580 nose and cockpit geometry*, in *Department of Mechanical Engineering*. 1999, Concordia University, Canada: Montreal.

[12] S O¨ zgen and Æ.M. Canıbek, *Ice accretion simulation on multi-element airfoils using extended Messinger model*. Heat Mass Transfer, 2009. **45**: p. 305-322.

[13] I Langmuir and K.B. Boldgett., *A mathematical investigation of water droplet trajectories*, in *AAF Technical Report 5418*. 1946.